AUTHOR QUERY FORM

Journal: Robotics and Autonomous Systems	**Please e-mail or fax your responses and any corrections to:** **E-mail: corrections.esch@elsevier.river-valley.com**
ELSEVIER **Article Number:** 2329	**Fax: +44 1392 285879**

Dear Author,

Please check your proof carefully and mark all corrections at the appropriate place in the proof (e.g., by using on-screen annotation in the PDF file) or compile them in a separate list. Note: if you opt to annotate the file with software other than Adobe Reader then please also highlight the appropriate place in the PDF file. To ensure fast publication of your paper please return your corrections within 48 hours.

For correction or revision of any artwork, please consult http://www.elsevier.com/artworkinstructions.

Location in article	Query / Remark **click on the Q link to go** Please insert your reply or correction at the corresponding line in the proof
Q1	Please confirm that given names and surnames have been identified correctly.
Q2	The language in this paper has been slightly changed. Please check for clarity of thought, and that the meaning is still correct, and amend if necessary.
Q3	Please check whether the edits made convey the intended meaning, and correct if necessary.
Q4	Please check whether the phrase "single-joint active orthoses" has to be changed as "single-joint active orthosis", and correct if necessary.
Q5	Please check whether the edit made conveys the intended meaning, and correct if necessary.
Q6	Please check whether the edits made convey the intended meaning, and correct if necessary.
Q7	The usage of 'Bode diagram' and 'bode diagram' needs to be consistent throughout the text. Please check, and amend as necessary.
Q8	Color statement has been added to the caption(s) of Figs. 8 and 9. Please check, and correct if necessary.
Q9	Please check the edit, and correct if necessary.
Q10	This sentence has been slightly modified for clarity. Please check whether the meaning is still correct, and amend if necessary.
Q11	Please check whether the term 'extend' can be changed as 'extent', and correct if necessary.
Q12	Please provide grant number for 'Fondazione Pisa' and 'Regione Toscana'.
Q13	Please check the journal titles given in Refs. [3,19–22,24,26,28,29,35,37,41,48].
Q14	lease check the term "post-Doc", and correct if necessary.
Q15	Would you consider changing the phrase 'She works' to 'She has been working' in the sentence "She... 2010"? Please check, and correct if necessary.
	Please check this box or indicate your approval if you have no corrections to make to the PDF file ☐

Thank you for your assistance.

ARTICLE IN PRESS
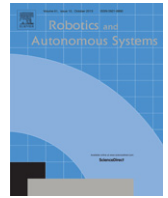
A light-weight active orthosis for hip movement assistance

Q1 Francesco Giovacchini [a], Federica Vannetti [b], Matteo Fantozzi [a], Marco Cempini [a], Mario Cortese [a], Andrea Parri [a], Tingfang Yan [a], Dirk Lefeber [c], Nicola Vitiello [a,b,*]

[a] The BioRobotics Institute, Scuola Superiore Sant'Anna, viale Rinaldo Piaggio 34, 56025, Pontedera (PI), Italy
[b] Don Carlo Gnocchi Foundation, via di Scandicci 256, 50143, Firenze, Italy
[c] Department of Mechanical Engineering, Faculty of Applied Sciences, Vrije Universiteit Brussel, Pleinlaan 2, B-1050 Brussels, Belgium

HIGHLIGHTS

- Development of a novel light-weight wearable powered bilateral pelvis orthosis.
- Design of a novel compact, light-weight series-elastic actuator (SEA).
- SEA closed-loop torque control bandwidth equal to 15 Hz.
- SEA output impedance ranges from 1 to 35 N m /rad in human gait frequency spectrum.
- The overall system usability was proved by tests with a healthy subject.

ARTICLE INFO

ABSTRACT

In the last decades, wearable powered orthoses have been developed with the aim of augmenting or assisting motor activities. In particular, among many applications, wearable powered orthoses have been also introduced in the state of the art with the goal of providing lower-limb movement assistance in locomotion-related tasks (e.g.: walking, ascending/descending stairs) in scenarios of activities of daily living. In this paper we present a light-weight active orthosis endowed with two series elastic actuators for hip flexion–extension assistance. Along with the description of its mechatronic modules, we report the experimental characterization of the performance of the actuation and control system, as well as the usability test carried out with a healthy subject. Results showed a suitable dynamic behavior of the actuation unit: the closed-loop torque control bandwidth is about 15 Hz and the output impedance ranges from about 1 N m/rad to 35 N m/rad in the frequency spectrum between 0.2 and 3.2 Hz. Results from the tests with the healthy subject proved the overall system usability: the subject could walk with the device without being hindered and while he received a smooth assistive flexion–extension torque profile on both hip articulations.

© 2014 Elsevier B.V. All rights reserved.

1. Introduction

Aging of the population is one of the most critical challenges Q2 current industrialized societies, characterized by a low birth rate and long life expectation, will face in the next years, and threatens the sustainability of our social welfare. In 40 years from now, nearly 35% of the European population will be over 60 year-old, resulting in the urgency to provide solutions enabling our aging

society to remain active, creative, productive, and – above all – independent [1,2].

Aging may cause reduced mobility, which leads to loss of independence [3–5]. According to the investigation accounted in [6], the spontaneous walking speed decreases by about 1% per year from age 60 onward, and the observed decline of maximum walking speed is even greater. Gait disorders and lower-limb impairments are also common and often devastating companions of aging [1–3]: several population-based studies showed a 35% prevalence of gait disorders among persons over age 70, and 80% over 85 years of age [4]. Gait disturbances have major consequences, including falls (leading to major fractures or head trauma), the number of which is expected to reach 500,000 by the year 2040 in US, representing a total annual cost of 16

* Corresponding author at: The BioRobotics Institute, Scuola Superiore Sant'Anna, viale Rinaldo Piaggio 34, 56025, Pontedera (PI), Italy. Tel.: +39 050 883 472, +39 338 681 2352 (Mobile).
E-mail address: n.vitiello@sssup.it (N. Vitiello).

billion dollars [7]. Senile gait disorders could also be an early manifestation of underlying pathologies, which might not only alter gait directly, but may also indirectly cause a subjective sensation of instability and insecurity, forcing individuals to adopt a more cautious gait [8–15].

A possible scenario for the next years is that aging-related gait syndromes will lead to an increase of the number of people needing assistance in their daily living activities, e.g. basic mobility, personal hygiene and safety awareness. In this scenario, it is plausible that people will become progressively more reliant on technology to meet their desire to live independently, actively and satisfactorily. Among all the assistive devices springing up, wearable robotic orthoses (namely "exoskeletons") were proposed as a solution by many research teams active in the field of medical robotics to assist people (mostly elderly) affected by gait disorders [16–18].

An exoskeleton for gait assistance is generally anthropomorphic in nature, "worn" by the user, and fits closely to his or her body [19]. Given the close interaction with the user, the robot should be light-weight and take into account the user's joints range of motion (RoM), anthropometry, and kinematics to provide a comfortable physical human–robot interface (pHRI) [20–22]. Furthermore, the actuation and control of the robot should allow the user to implement his or her own movement without hindrance while receiving a certain assistance safely: in this framework, a very efficient and often adopted design methodology foresees the endowing of a mechanical compliance between the exoskeleton actuators and the user/robot interface, the so-called Series Elastic Actuator (SEA) strategy [23].

Many robotic exoskeletons can be found in the current state of the art: the broad variability in mechatronic design, control and human–robot interface [19] of these devices is due to differences in the targeted end users and expected usage. Some of them have been designed as unilateral support, in order to assist post-stroke patients. ALEX is a leg exoskeleton whose hip and knee joints are powered by linear actuators [24], controlled by means of an adaptive impedance controller: it is worth to note that ALEX is the only lower-limb exoskeleton which provides passive degrees of freedom (DoFs) allowing vertical and lateral movement of the pelvis, thus a more natural gait pattern. Sawicki et al. [25] investigated on ankle–foot and knee–ankle–foot orthoses powered by McKibben-type pneumatic muscles, which provide an inherent transmission compliance, but with the drawback of requiring a double actuation (antagonistic actuators arrangement). Recently, at Vrije Universiteit Brussel (Brussels, Belgium), a knee–ankle foot orthosis has been developed and tested [26]: in this case pleated pneumatic artificial muscles were used as actuators and a proxy-based sliding mode strategy ensured a safe human–robot interaction. A huge number of bilateral active orthoses have been presented, as well. Relevant bilateral orthoses for post-stroke patients are the LOKOMAT [27] and the LOPES [28], the latter being introduced as the first lower-limb exoskeleton with inherently compliant joints. The LOPES is indeed capable of a high assistance while keeping a low output impedance, thanks to its SEA actuation strategy [28]. Wearable devices for paraplegic or hemiplegic rehabilitation, aiming at replacing locomotion in case of no residual mobility, are the Vanderbilt powered limb orthosis [29] and HAL, an active suit for motion assistance commercialized by Cyberdyne (Tsukuba, Japan) [30]. Other exoskeletons have been specifically designed for assisting the cautious gait of elderly people, such as the exoskeleton EXPOS reported in [31], while other researches focused on devices for body weight support, such as the Moonwalker [32] and the Bodyweight Support Assist by Honda (Honda, Tokyo, Japan). Furthermore, lower-limb exoskeletons were also designed for augmenting human strength, enabling to carry heavy loads, mainly for military purposes: well-known examples are the BLEEX [33], the SARCOS exoskeleton (Sarcos, US) and the MIT passive exoskeleton [34], all developed within the frame of the DARPA program Exoskeletons for Human Performance Augmentation (EHPA, [19]).

It is worth to cite also single-joint active orthoses, such as the SERKA, an active knee orthosis addressing stiff knee gait in stroke patients [35] actuated by a cable-driven rotational SEA, the Dynamically Controlled Ankle–Foot Orthosis [36] and the Adaptive Ankle–Foot Orthosis by Blaya et al. [37], which are examples of simpler active orthoses making use of SEAs to assist push-off or to correct dropped foot gait. Examples of active orthoses for the hip flexion–extension assistance are the devices introduced by do Nascimento et al. [38] and the hip exoskeleton designed by Ferris et al. [39], both powered by artificial pneumatic muscles, and the Stride Management Assist by Honda (Honda, Tokyo, Japan).

In this paper, we introduce the design of a light-weight active pelvis orthosis (APO), which was preliminary presented in [40], for assisting hip flexion–extension (Fig. 1). The device was conceived with two innovative solutions. Firstly, it has a novel, compact and light-weight SEA unit which exploits a custom torsional spring. Secondly, we proposed an optimized design based on extremely light-weight carbon-fiber linkages, embedding manual adjustments for fitting the orthosis to a wide range of user sizes, and passive DoFs which follow the gait motions out of the flexion/extension plane (pelvis tilting, thigh abduction). The device hence ensures good kinematics compatibility, enhancing the comfort of the human–robot physical interaction, avoiding limitations and constrains to user's gait pattern, and addressing the match of intra- and inter-subject anthropometric variability.

Along with the description of the mechatronic modules of APO, this paper also reports its experimental characterizations. In particular, the performance of dynamic response of SEA, and overall usability of the system in a gait assistance task. The usability is tested by controlling APO with an adaptive motion control strategy which was early introduced in [17,18].

The paper is structured as follows: Section 2 describes the design of the light-weight active orthosis. Results of the experimental characterization are reported in Section 3 and discussed in Section 4 Finally, Section 5 draws the conclusions.

2. Mechatronic design

This section presents the main technical solutions of the active orthosis we conceived for the APO system. Hereafter we describe the three subsystems we developed: namely the mechanical structure, the actuation unit and the control system.

2.1. Mechanical structure

The device is sustained by an horizontal C-shaped frame, surrounding the user hips and the back of the pelvis, and interfaced to the trunk by means of three orthotic shells (two lateral and one rear); the frame carries the two actuation units. The structure is realized in two 2.5 mm thickness carbon-fiber lateral arms, connected through a rear straight bar. The rear bar is composed by an external guide in which two internal rods can slide: the bar length can then be adjusted in order to match the distance between the two lateral shells, ensuring the frame to be tightly attached to the upper body in the medial–lateral direction (Fig. 2(a)). One of the two sliding rods can be locked by a fast-detach pin (for coarse regulation and fast don–doff procedure), and finely adjusted thanks to a leadscrew mechanism. In order to further make easier the wearing procedure the structure can be also completely separated into two parts (right and left).

The human and robot hip flexion–extension axes are aligned in the sagittal plane thanks to the adjustment of the horizontal and vertical positions of the rails in the cuff-frame interface.
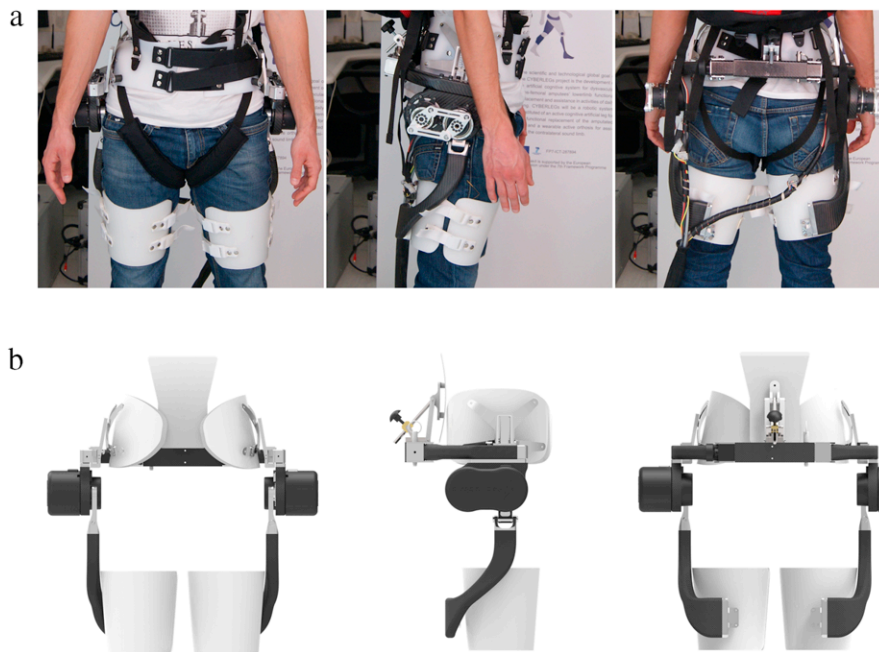
Fig. 1. Overview on the APO. (a) Frontal, lateral and back view of APO worn by a healthy subject. (b) Frontal, lateral and back view of the APO CAD model.
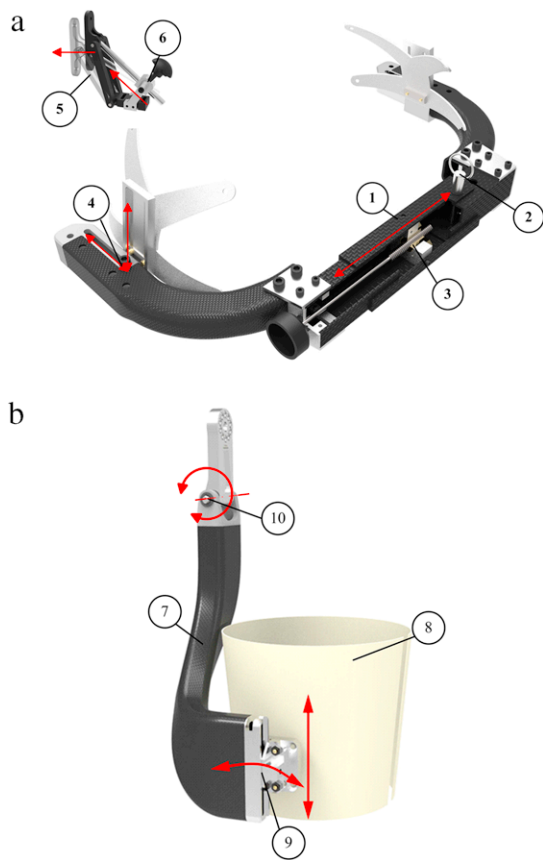
Fig. 2. Overview of APO subsystems. (a) C-shaped frame connected to user's trunk. (1) Rear bar connecting the two carbon-fiber arms. (2) Detachable pin for regulation. (3) Leadscrew mechanism for fine adjustment. (4) Rails for flexion–extension axes alignment. (5) Back support interface with the subject back, namely lumbar region. (6) Screw mechanism for adjustment. (b) Thigh linkage. (7) Carbon-fiber linkage. (8) Orthotic shell interfaced with user's thigh. (9) Sliding and rotational adjustment of the orthotic shells. (10) Passive adduction–abduction rotational axis.

Furthermore the back orthotic shell is fixed on the rear bar and adjusted by a screw mechanism to assess a correct and ergonomic

pushing support on the lumbar region of the subject (Fig. 2(a)), for a correct transmission of the assistive torque. The entire subsystem reaches a total weight of 0.8 kg.

The actuated axes drive two carbon-fiber links shown in Fig. 2(b), molded with a shape sweeping from the lateral to the back side of the thigh. The carbon fiber thickness is 2 mm; this structural optimization leads to the production of light-weight links (less than 0.3 kg for each one) while the necessary structural stiffness is still preserved. The carbon composites are coupled to the rest of the mechanics by means of aluminum inserts glued to the carbon fiber through a bi-component epoxy resin (Scotch-Weld^{TM} 9323 - 3M^{TM}, Milan, Italy). The inserts at the interface between carbon-fiber and metal components (the thigh links and the trunk support parts) are provided with slots, that guarantee the needed regulations towards a comfortable wearing and the human–robot joint axes alignment (Fig. 2(b)).

The shape of the links allows to swap them in the exoskeleton assembly, connecting the actuation axes with the front side of the thigh, without affecting the functionality. This additional possibility may be useful in those cases in which the rear part of the thighs needs to be kept free from any component, for instance to allow the user to sit without hindrance.

Thigh links are also endowed with a passive rotational DoF for abduction–adduction: this joint is located in a distal position with respect to the flexion–extension joint (60 mm below): this choice allows the abduction–adduction passive DoF to be not loaded by the weight of the actuation unit. Although the rotation axis of this passive DoF is not aligned with the one of the human joints, it still contributes to provide a comfortable interaction and a not rigid constraint of the user leg while walking.

In order to comply with different lower-limb lengths, the vertical position of the two plastic orthotic shells, which encircle the user's thigh, is adjustable thanks to lockable sliders situated at the tip of the carbon fiber linkages (Fig. 2(b)). These lockable sliders are endowed with a further regulation: it is possible to rotate the shells with respect to the linkage to find the most comfortable position for each user.

The APO physically interfaces with the user's body in five zones: the three thermo-shaped orthotic trunk shells stabilize the frame over the user's waist, and the two upper-leg shells are tightened
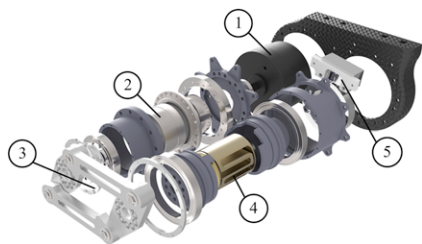
Fig. 3. Exploded view of the series elastic actuation unit. (1) DC motor with embedded incremental encoder. (2) Harmonic Drive. (3) 4-bar transmission mechanism. (4) Torsional spring. (5) Absolute encoder.

Fig. 4. APO passive and active DoFs. (a) Height regulation of the thigh orthotic shell, range of user's trunk dimensions and RoM of passive adduction–abduction DoF. (b) Human–robot joint axis alignment on lateral and sagittal plan, adjustment of trunk's orthotic shell on lateral plan and RoM of active flexion–extension DoF.

around the thighs by means of elastic belts. This solution should guarantee a comfortable interaction and a safe transmission of the assistive torque by preventing the human–robot interaction surfaces from slippages. Moreover, the use of a soft orthopedic material and a wide contact area contribute to reduce and distribute the pressure on the user's skin. In addition, two straps allow a portion of the APO weight to be supported by the shoulders, and thus avoid the trunk from being loaded with an excessive lateral pressure.

All the orthotic shells were custom manufactured with a two-layered structure: a 3 mm-thick internal layer of thermoplastic polyethylene foam (Plastazote® 617S7, Otto Bock, Duderstadt, Germany), for moisture draining and skin transpiration, and a 3 mm-thick outer layer of polypropylene (ThermoLyn® Polypropylene 616T20, Otto Bock, Duderstadt, Germany). These shells come in different sizes, and can also be tailor-made on each subject.

2.2. Actuation units

APO is endowed with two actuation units, one for each hip flexion–extension joint (Fig. 3), mounted on the lateral arms. The actuation unit employs a series elastic actuator (SEA) architecture [22]. SEAs have been successfully applied in the field of wearable powered robots mostly to solve safety issues and reduce the inherent output impedance [41–43]. In this case, the actuation is not rigid and allows minimum joint output impedance across the frequency spectrum of gait. Furthermore, variations in the output impedance can still be achieved by means of closed-loop interaction control strategies [41–43].

The motor units have been designed taking as reference the hip angle and torque profiles reported by the Winter dataset: in particular we assumed a natural cadence of 105 steps/min and a user weight of 80 kg [44]. The target amount of assistance was set to 50% of the human torque required during ground-level walking: hence, the actuator was designed in order to provide a maximum torque of 35 N · m.

The SEA in-series elasticity was realized by a custom torsional spring, which achieves a stiffness of 100 N · m/rad — a value comparable with the human hip average stiffness during ground-level walking [45] — and bears the torsion stress up to the design value without neither yielding, nor presenting hysteretic or non-linear behavior. The spring compliance prevents the subject from an uncomfortable (or even painful) interaction with an excessively stiff device in case of high-frequency movements (e.g. sudden spasms, interaction with the ground). The same spring has been used to design the actuation unit of the NEUROEExos elbow exoskeleton developed at The BioRobotics Institute (Scuola Superiore Sant'Anna, Pisa, Italy), and its design and experimental characterization were already presented in [46].

With reference to Fig. 3, each actuation unit is deployed around two parallel axes. One is the axis of the 100 W DC motor (EC60, Maxon Motor®, Sachseln, Switzerland) equipped with an incremental encoder (1024 ppr, MILE, Maxon Motor®, Sachseln,
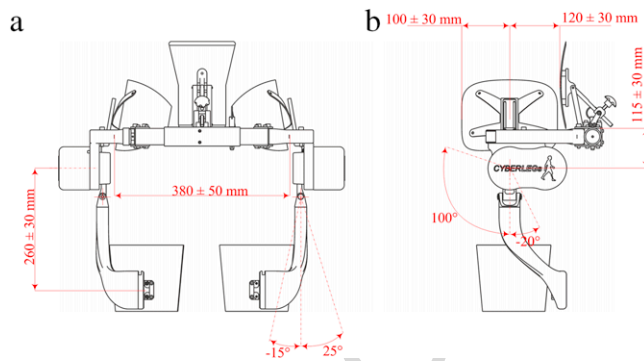
Switzerland) and coupled with a 80:1 Harmonic Drive (HD) (CPL-17A-080-2A, Harmonic Drive®, Limburg, Germany) reduction stage. On the other axis (which is the one actually collocated with the human hip flexion–extension axis) there is the torsional spring in series with a 32-bit absolute encoder (RESOLUTE™, ring: RESA30USA052B, read head: RA32BAA052B30, Renishaw®, Gloucestershire, England), which measures the absolute hip joint angle. Each actuation unit reaches a weight of 1.2 kg. By assuming a range of movement of the human hip joint from −20° (minimum extension angle during walking) to 90° (maximum flexion angle in a seated position), we opted for a transmission means between the two parallel axes based on a 4-bar mechanism, with a range of motion between −30° and 110° (Fig. 4(b)), limited by emergency mechanical stops. The two-axis configuration was chosen in order to reduce the overall lateral encumbrance, namely 110 mm, due to the length of the gear-motor unit and of the torsional spring. Although this encumbrance is relatively small, this solution is a limitation of the current design as it partly prevents the user from swinging his or her arms. However, its encumbrance is comparable to the one of other lower-limb exoskeletons [19].

The entire system has a total weight of 4.2 kg (this weight excludes the control unit which is still remotely located in this prototype) and the adjustable DoFs allow the system to comply with a wide range of user's body size (Fig. 4).

2.3. Control system

The APO control system is based on a hierarchical architecture that comprises a *low-level torque control* layer (two independent torque controls, one for each actuation unit) and a *high-level* layer implementing an adaptive assistive strategy (Fig. 5(a)).

(1) *Low-level torque control*: the low-level controller is in charge to manage the actuators in order to track the set torque value to the moving linkage of the exoskeleton. The closed-loop control architecture is that of a classical proportional–integral–derivative (PID) regulator (Fig. 5(b)). The PID regulator operates on the error between the desired torque τ_{des} and the measured torque τ, and returns an electrical current provided to the motor, within a saturation interval of ±3.2 A corresponding to a torque range of ±35 N · m. The motor current is controlled by means of a commercial servo amplifier (EPOS2 70/10, Maxon Motor®, Sachseln, Switzerland). As it is explained in [22], bandwidth of a SEA system controlled by means of a PID compensator can be limited by design. Thus, PID regulator coefficients were tuned manually to achieve the widest closed-loop bandwidth, as will be shown in Section 3.2 with the characterization of the controller.

The measured torque is estimated from the deformation of the torsional spring by means of the two encoders (respectively
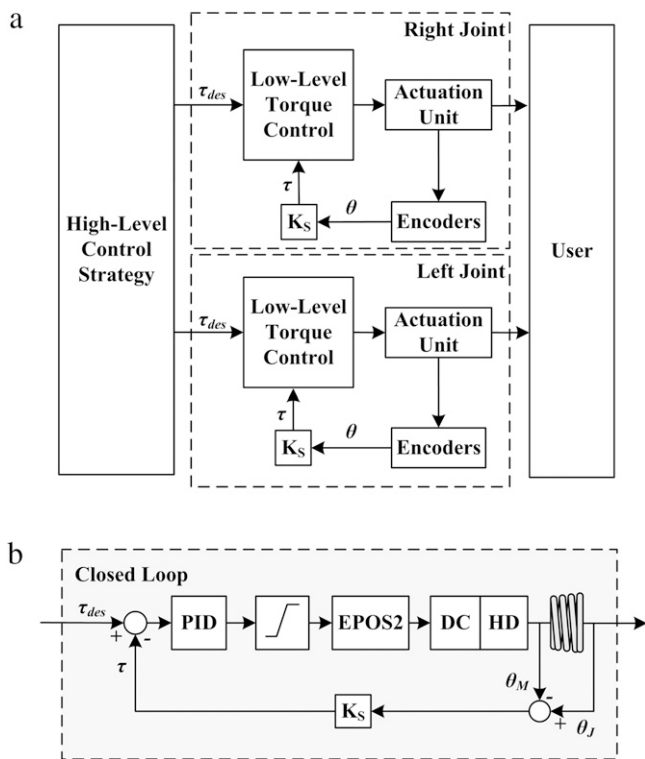
Fig. 5. Scheme of the control system of APO. (a) Block diagram of the hierarchical control architecture. (b) Low-level closed-loop torque control.

measuring the Harmonic Drive output shaft angle θ_M and the joint angle θ_J, the torsional stiffness K_S being known. Since one of the two encoders is incremental (the one on the motor side), an initializing procedure was needed at the power-on of the system, in order to correctly acquire the reference zero value of spring deformation, corresponding to a null transmitted torque: this was achieved through a rigid pin, bypassing the torsional spring (impeding its deformation and then keeping it unloaded) during the exoskeleton starting, which was then removed after initialization of the incremental encoder reference value.

(2) *High-level assistive control*: in order to be used as a wearable active orthosis for human motion assistance, the torque control should be able to provide the user with the assistive torque with near-zero output impedance, i.e. with minimum to null joint parasitic stiffness [43]. Aiming at the system usability in a task of gait assistance, we opted for a high-level control strategy that could provide a desired torque reference variable over the stride. This way we could assess whether the closed-loop torque control bandwidth was sufficiently large and the parasitic output stiffness sufficiently low to allow the system to track the desired torque with a relatively small error, at different gait speeds. As an assistive control strategy we selected a model-free (it does not require any *a priori* knowledge about the gait dynamics) algorithm presented in a recent work by Ronsse et al. [18]. This algorithm has been used to provide users of the LOPES exoskeleton with hip flexion–extension assistance, and it relies on the use of adaptive oscillators (AOs), which are mathematical tools introduced by Righetti et al. [47] that – when coupled with a kernel-based non-linear filter – can constantly track and provide a zero-delay estimate of a non-sinusoidal periodic signal (e.g., hip or knee angle profile during gait), even when it slowly changes its main features such as frequency and envelope over cycles [18,48,49]. While a detailed analysis of the mathematical formulation of the algorithm is available in [18], hereafter we briefly recap its working principle and how we implemented it on the APO.

Adaptive oscillators are a set of non-linear differential equations with the capacity to synchronize with an input periodic signal, not by tracking its current value, but rather tracking the signal periodicity characteristics (i.e. amplitude, frequency and lead phase). When implemented in the dynamic system controller, the synchronization capability of adaptive oscillators can be exploited to learn the phase of gait of the subject accomplishing a ground-level walking task. For the APO high-level control we used a modified version of an Hopf oscillator as AO, and a set of 60 Gaussian functions as kernel of the non-linear filter. Thanks to the capability of this architecture to – instead of doing mere synchronization – learn the frequency (and then the phase) and the envelop of a quasi-periodic teaching signal, we could track and learn the quasi-periodic behavior of each hip joint angle, and provide a reliable prediction of the joint angle vs. gait phase within the gait cycle. This means that at each gait phase φ the AO and the non-linear filter can provide an estimate of both the hip joint angle $\hat{\theta}_J(\varphi)$ and its future value at a phase $\varphi + \Delta\varphi$, namely $\hat{\theta}_J(\varphi + \Delta\varphi)$, being $\Delta\varphi$ a phase lead tunable by the experimenter. The assistive torque is then computed by setting the $\tau_{des} = K_v \cdot [\hat{\theta}_J(\varphi + \Delta\varphi) - \hat{\theta}_J(\varphi)]$, being K_v a tuneable virtual stiffness. This way the user's joints are smoothly attracted towards their future positions by means of an attractive virtual stiffness field, while leaving the opportunity to the user to constantly change the frequency and shape of his or her gait pattern.

(3) *Control unit and safety loop*: The control system runs on a real-time controller, a cRIO-9082 (National Instruments, Austin, Texas, US), endowed with a 1.33 GHz dual-core processor running an NI real-time operating system and a field programmable gate array (FPGA) processor Spartan-6 LX150. Both the high- and low-level layers run at 1 kHz.

The APO control system implements a safety loop that switches off the actuation when the measured torque is higher than 30 N·m, or the joint speed is greater than 400° · s⁻¹. In addition, both the experimenter and the user can turn off the apparatus by means of a red, emergency button.
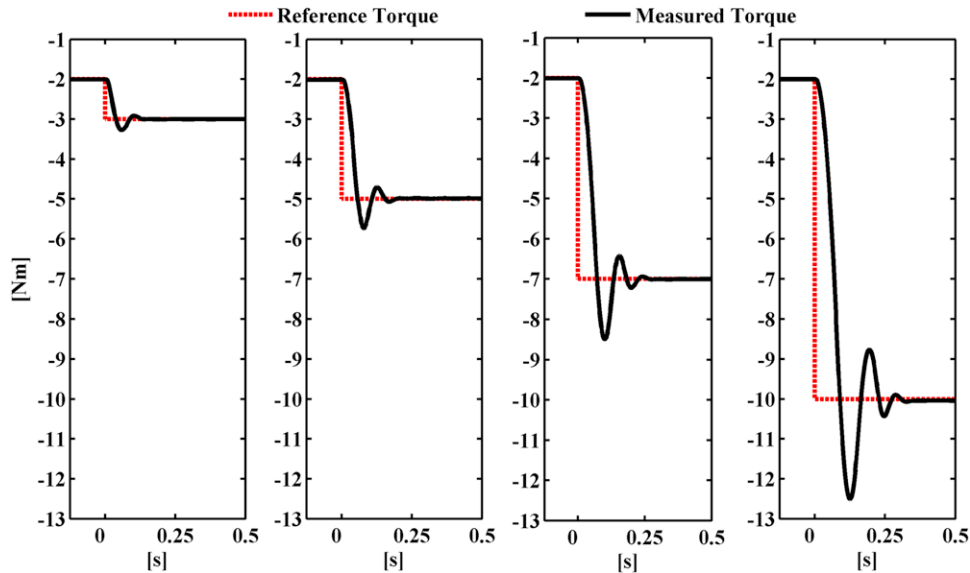
3. Experimental characterization

In this section we describe some experimental sessions carried out to characterize the performance of the hierarchical control system depicted in Section 2.3. First, in order to characterize the closed-loop torque control performance, we analyzed the response of the exoskeleton system alone, with commanded torque step and chirp in joint stationary conditions (namely with the joint velocity being equal to zero), and then we assessed the joint output impedance in dynamic condition. Second, one healthy subject volunteered to walk with the APO under two conditions, namely *transparent mode* (TM, the desired torque of each joint was set to zero), and *assistive mode*(AM, the desired torque of each joint was calculated based on the above high-level control strategy).

3.1. Characterization of the closed-loop torque control

In this subsection, we will describe the test assessing the performances of the lower control layer.

(1) *Step response*: performance of the closed loop controller has been assessed by recording the responses to different amplitude steps of desired torque. The moving linkage of the exoskeleton was driven to a mechanical stop, and pressed against it with an initial commanded torque value of $\tau_{des} = -2$ N · m. Then several trials were conducted, with four different signal steps in the range $\Delta\tau_{des} \in [-1, -8]$ N · m superimposed to the initial steady torque; each step was repeated 15 times for statistical reproducibility of the experiment. The averaged responses are shown in Fig. 6

Fig. 6. Experimental characterization of the step response for different desired step amplitudes. Each graph reports the reference torque (red dotted line) and the averaged responses over 15 iterations (black line).

Table 1

Average and standard deviation of step response characterization.

Step amplitude [Nm]	Rise time [s]	Settling time [s]	Max. overshoot [N · m]
1	0.0188 ± 0.0004	0.0630 ± 0.0001	0.2752 ± 0.0028
3	0.0271 ± 0.0007	0.1089 ± 0.0003	0.7386 ± 0.0057
5	0.0467 ± 0.0006	0.1367 ± 0.0006	1.4925 ± 0.0213
8	0.0727 ± 0.0016	0.1761 ± 0.0013	2.5082 ± 0.0517

and average values of the rise time, settling time and maximum overshoot are reported in Table 1 for each step amplitude. The torque control shows a relatively fast underdamped behavior, which slightly changes with the increase of the step value. Indeed, the rise time, the settling time and the overshoot increase with the step amplitude, respectively from 0.018 s to 0.072 s, from 0.06 s to 0.17 s, and from 0.27 N · m to 2.50 N · m. This non-linear behavior is caused by the saturation of the electrical current driven by the EPOS2, which limits the maximum acceleration of the DC motor shaft. Anyhow, performances are satisfactory for our purposes, the system responding timely and stably to sudden variation.

(2) *Chirp response*: the frequency response of the torque control was characterized by recording the exoskeleton joint response to a linear torque chirp (frequency 0–20 Hz, duration 300 s, and amplitude 4 N·m). The test was repeated seven times for improving the estimate of the Bode diagram (amplitude and phase) of the system $G(s) = \tau(s)/\tau_{des}(s)$. The resulting amplitude Bode diagram of the chirp response is reported in Fig. 7(a), and the estimated −3 dB bandwidth was about 15.5 Hz, which is sufficiently high for providing assistance to the movement of lower limbs.

(3) *Output impedance*: in the field of assistive robotics, one of the more demanding features for a safe and reliable power transfer towards the user is the transparency of the actuated joint axes with respect to the wearer natural movement. No hindrance should be applied by the device while accomplishing a motion task. The joint output impedance represents a measurement of the level of transparency of a human interacting with a mechanical device [43]: mechanical impedance is defined as $Z(s) = \tau(s)/\theta(s)$ where $\theta(s)$ is the Laplace transform of the applied angular displacement and $\tau(s)$ the Laplace transform of the resulting torque on the rotational axes. We characterized the output impedance of the APO under zero-torque mode, i.e. when the orthosis is asked to follow

the intentional movement of the wearer without constraining the free-motion [43]. Parasitic output impedance was evaluated by moving manually the linkage, and recording the angular displacement and the SEA torque. The experimenter displaced the APO joint with a quasi-sinusoidal flexion–extension motion of amplitude 20°. The frequency of the movement varied quasi-linearly in the range 0.2–3.2 Hz for a recording session of 100 s. Five iterations were repeated for a more consistent statistical analysis. Fig. 7(b) shows the profile of the resistive torque felt by the subject during the task, along with the profile of the flexion–extension angle. The interaction torque amplitude increases with the motion frequency, reaching a peak of 5 N · m for 3.2 Hz movement. Fig. 7(c) shows the Bode plot of the transfer function from the joint angle to the measured torque. The system shows low output impedance over the typical bandwidth of the human motion, meaning that if the user wants to walk while wearing the APO, the exoskeleton would exert a minimal resistive load, preventing him or her from additional muscular efforts. Under the action of the zero-torque control the joint output impedance resulted lowered with respect to the inherent passive stiffness of the joint torsional spring — about 100 N·m/rad. Values ranged from about 1 N·m/rad (−40 dB) for a motion within 0.2 and 1 Hz, to about 35 N · m/rad (−9.11 dB), at the peak frequency of 3.2 Hz.

3.2. Characterization of the high-level control

In order to evaluate the functionality of the APO system, a prototypical task of gait assistance was designed and tested on a healthy volunteer (male, 30 years old, 70 kg). The experiment was carried out at the premises of Don Carlo Gnocchi Foundation (Florence, Italy). The healthy subject was requested to walk on a treadmill for about 2 min at four different velocities (from 2 to 5 km/h) under both the TM and AM modalities. For the AM session we set the virtual stiffness at either $K_v = 15$ N · m/rad or $K_v = 20$ N·m/rad, respectively for the gait velocity being equal or higher than 2 km/h. The phase lead was set to $\Delta\varphi = 0.628$ rad.

For each gait velocity and for both AM and TM modalities, we recorded the joint angle and SEA torque of the left and right legs. Collected data were segmented into gait cycles: variables of each stride were in turn resampled between 0 and 100% of the gait cycle. From the collected variables we derived the joint velocity and SEA power. It is worth noting that we assumed that the joint angle θ_J
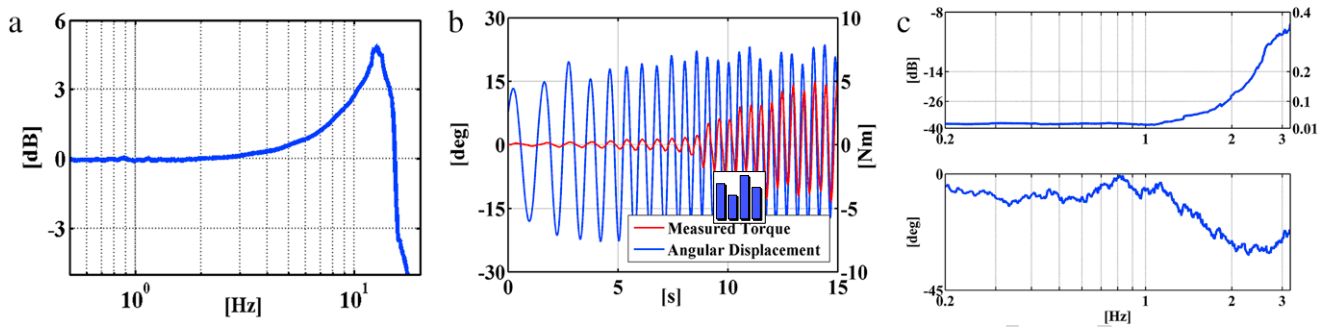
Fig. 7. Experimental characterization of the torque control. (a) Chirp response: amplitude bode diagram of the transfer function from desired torque to measured torque. (b) Characterization of the joint output impedance: angular displacement and interaction torque. (c) Amplitude (normalized with respect to the value of the inherent compliance of the series elasticity) and phase Bode diagram of the transfer function from angular displacement to interaction torque.

Table 2
Average and standard deviation of RMSE between desired and measured torque during walking under the TM and AM conditions. Data are computed for both the right and left hip joints.

	Gait speed	2 km/h	3 km/h	4 km/h	5 km/h
Right hip joint	TM RMSE [N m]	0.160 ± 0.098	0.171 ± 0.044	0.286 ± 0.022	0.478 ± 0.073
	AM RMSE [N m]	0.245 ± 0.011	0.516 ± 0.031	0.703 ± 0.114	1.152 ± 0.231
Left hip joint	TM RMSE [N m]	0.148 ± 0.066	0.164 ± 0.027	0.235 ± 0.017	0.426 ± 0.064
	AM RMSE [N m]	0.223 ± 0.010	0.474 ± 0.032	0.638 ± 0.057	0.902 ± 0.170

is null when the person is standing still with his or her legs fully stretched, and it is positive when the hip is flexing (namely $\dot{\theta}_J > 0$ when the hip joint is flexing; $\tau > 0$ means that the SEA is applying a flexing torque onto the human hip joint).

Figs. 8 and 9 show the average curves with the standard deviation contour of the collected/computed variables for the TM and AM sessions respectively. The overall usability of the APO in a prototypical task of walking was demonstrated by three experimental evidences. The first point is that the torque control has a suitable performance also in the case of $\dot{\theta}_J \neq 0$, both in TM and AM modalities. The RMSE under TM was in the worst scenario, namely at 5 km/h equal to about 0.4 N · m (for both right and left legs). This result proves that in addition to a wide closed-loop bandwidth the closed-loop control can also rapidly reject disturbances deriving from the joint movement: this is a key point that allows the user to wear and walk (under TM) with the exoskeleton without any additional effort for his/her musculoskeletal system. The maximum parasitic torque reaches a negative peak of about -1.5 N · m when the subject walks at 5 km/h, more precisely in correspondence of the swing phase of both legs, namely when the joint velocity has a positive peak. As a consequence this is also the case in which the SEA power has a negative peak, which reaches about -5 W: this is case of maximum hindering which the APO applies to the movement of the user. Nevertheless, a negative power peak of -5 W, and an average negative power of -0.45 W (as shown by Fig. 8 and data reported in Table 3), is indeed less than 1% of the maximum flexion–extension torque powered by the hip muscles of a 75 kg healthy subject during a ground-level walking task at normal cadence [44]. A similar analysis can be done for the AM condition. Under the AM, while the gait pattern in terms of range of motion, joint velocities and angle profile over the gait cycle does not differ from the TM session, data shown in Fig. 9 point out that: (i) the range of the assistive torque spreads as the gait speed increases; at 5 km/h the assistive torque over the cycle oscillates between -8 N · m and 10 N · m; (ii) the SEA power is mostly positive and the peak value in correspondence of the middle-swing phase increases from about 20 to 40 W with the gait speed increasing from 2 to 5 km/h.

In order to quantitatively assess the performance of the torque control in dynamic conditions (namely $\dot{\theta}_J \neq 0$), for both AM and TM modalities, we computed the root means square error

(RMSE) between the desired and the actual joint (data from right and left joints were analyzed separately in order to assess any potential asymmetrical behavior between the two joints). Results are summarized in Table 2. For the TM and AM conditions, the RMSE increased respectively from 0.14 ± 0.06 N · m and 0.22 ± 0.01 N·m, when the gait speed is 2 km/h, to 0.47 ± 0.07 and 1.15 ± 0.23 N · m, when the gait speed is 5 km/h. Results clearly show how the RMSE between the measured and the desired torque is higher in AM condition than in TM conditions. This fact is explained as follows: under TM condition, the RMSE between measured and desired torque corresponds to the estimate of the parasitic residual torque exerted by the robot on the limb, when the desired reference torque value is a null constant. This variability across stances is due to the low-level controller performances, and to the non-perfect repetition of the gait steps. In AM utilization, this background variability is superimposed on the one due to the fact that the high-level oscillator locks with the current phase of the gait pattern, and extrapolates a reference torque signal on its basis. As a consequence, a higher RMSE is returned.

In this case the RMSE between the desired and actual torque in the worst scenario is about 1 N · m, which is in the range of 10% of the maximum commanded torque. This is a proof that the system can successfully implement an assistive strategy: the controller has the capability of tracking a desired torque reference variable along the gait cycle. Furthermore, a remarkable point is that from the analysis of the performance of the actuation units powering the right and left sides we derive that the APO has a quite symmetrical behavior. The maximum difference in the RMSE is 11% and 21% while walking at 5 km/h, respectively under the TM and AM conditions.

In order to quantitatively assess the mechanical power transferred from the exoskeleton to the user, for both AM and TM modalities, we computed the mean value of the SEA power (data from the right and left joints were analyzed separately in order to assess any potential asymmetrical behavior between the two joints). Results are summarized in Table 3 and shown in Fig. 9. For the TM the mean power is about null, and ranges from -0.081 ± 0.05 W, when the gait speed is 2 km/h, to -0.36 ± 0.10, when the gait speed is 5 km/h. On the other hand, for the AM session the mean power ranges from 4.9 ± 0.29 W, when the gait speed is 2 km/h, to 10 ± 0.43 W, when the gait speed is 5
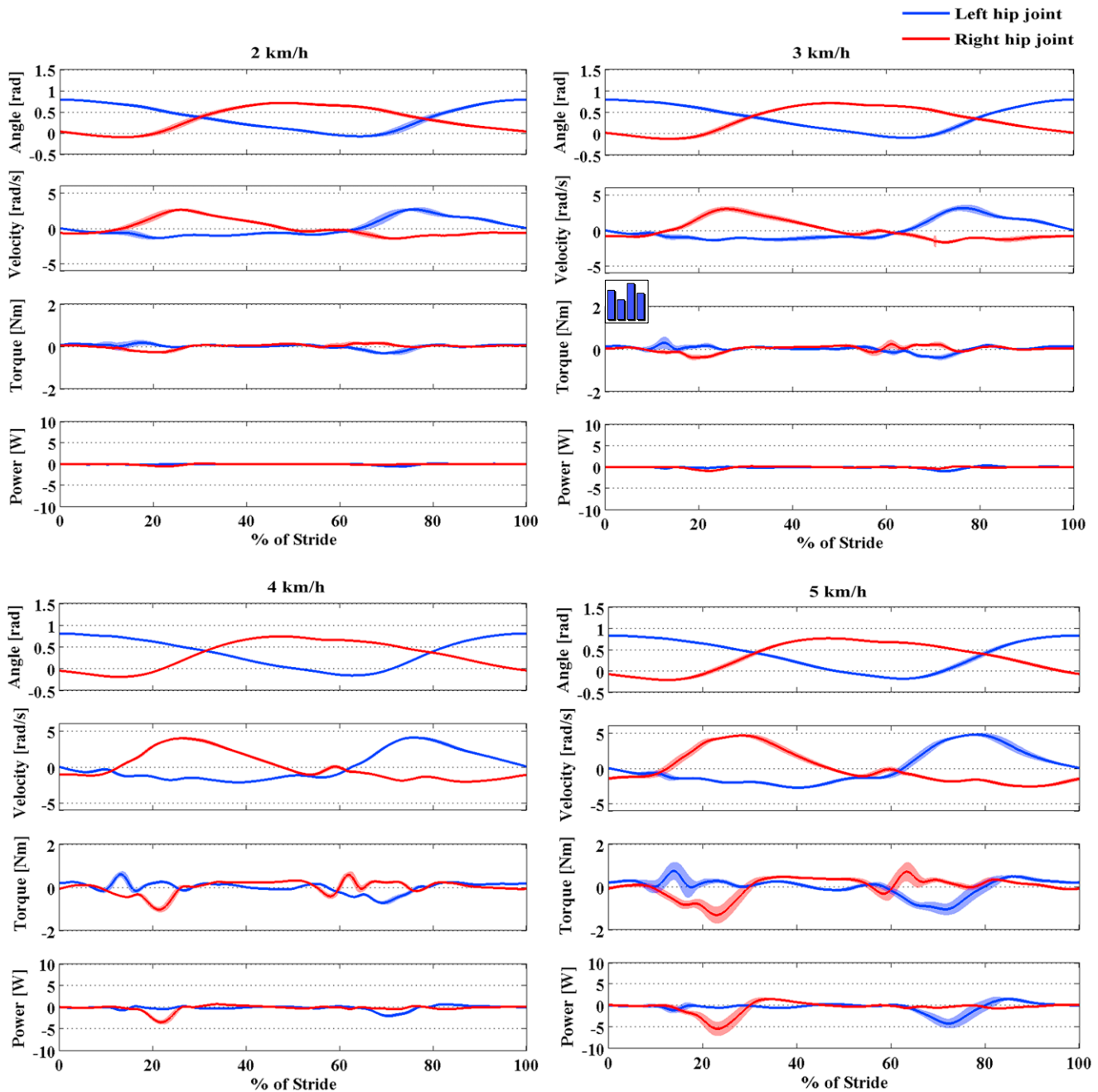
Fig. 8. Walking with the APO under TM. For each gait speed, the following variables for left and right hip joints are averaged over all strides and plotted against the percentage of the stride cycle: hip joint angle, hip joint velocity, SEA torque and power. For each graph the average curve (solid line; blue for left and red for right joint) is shown along with the standard deviation contour. (For interpretation of the references to color in this figure legend, the reader is referred to the web version of this article.)

Table 3
Average and standard deviation of the gait-cycle mean value of the SEA power during walking under the TM and AM conditions. Data are computed for both the right and left hip joints.

	Gait speed	2 km/h	3 km/h	4 km/h	5 km/h
Right hip joint	TM Power [W]	-0.088 ± 0.103	-0.104 ± 0.098	-0.182 ± 0.026	-0.445 ± 0.138
	AM Power [W]	5.253 ± 0.228	6.389 ± 0.393	7.913 ± 0.310	10.008 ± 0.438
Left hip joint	TM Power [W]	-0.081 ± 0.056	-0.096 ± 0.051	-0.128 ± 0.015	-0.359 ± 0.107
	AM Power [W]	4.902 ± 0.297	5.938 ± 0.471	7.865 ± 0.324	9.490 ± 0.430

km/h. This results prove that the APO under the action of an assistive strategy can actually transfer mechanical power to the user. It is worth noting that with the increase of the gait velocity the amount of power (both mean and peak value) applied by the APO to the human hips increases. This is simply a consequence of the fact that with the increase of the gait velocity, there is an increase of the gait stepping and hip joint velocity during the swing phase. When moving from the TM to the AM condition, the major features of the gait pattern are not altered by the applied assistive torque: the device transfers mechanical power to the human limb
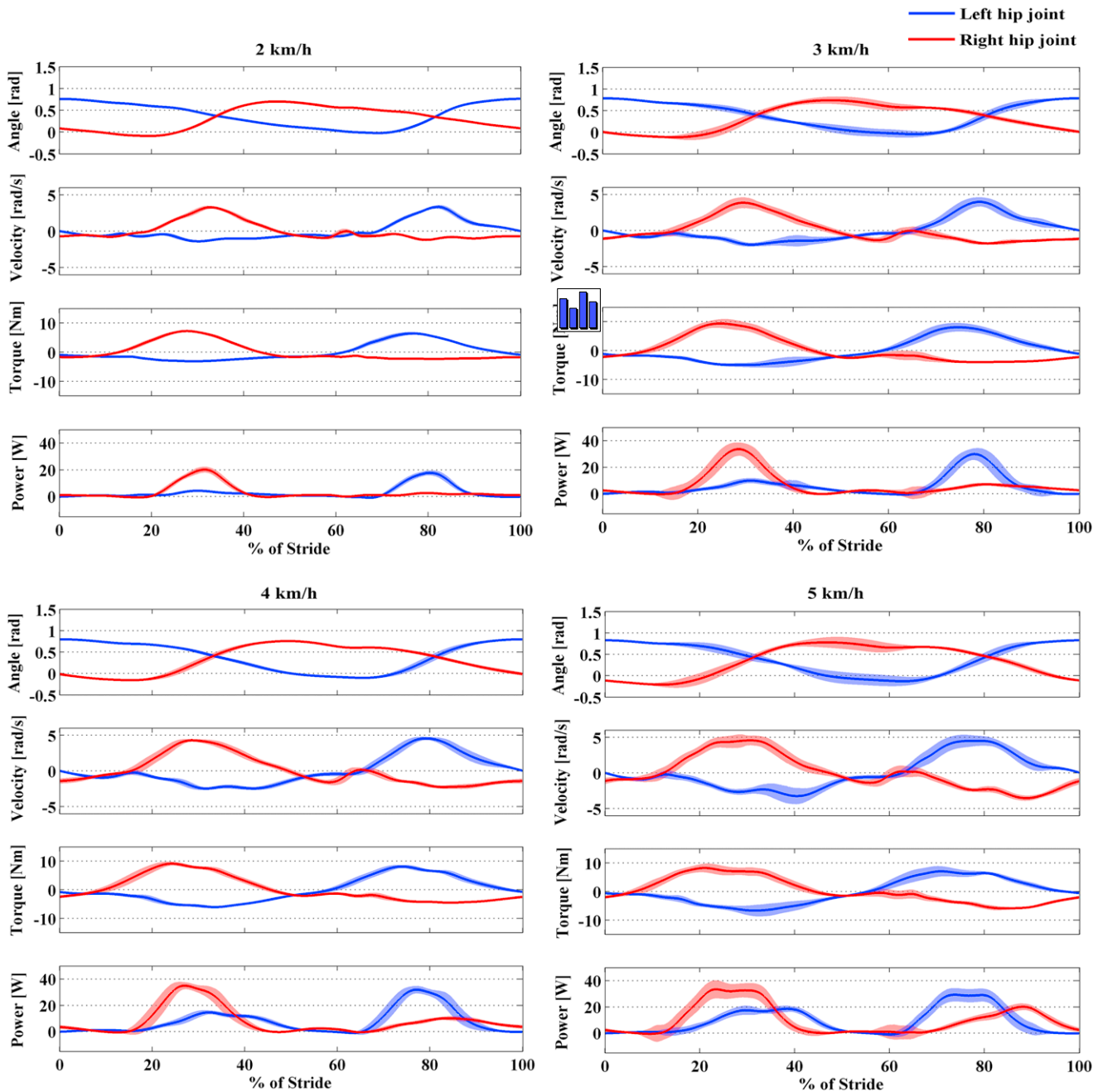
Fig. 9. Walking with the APO under AM. For each gait speed, the following variables for left and right hip joints are averaged over all strides and plotted against the percentage of the stride cycle: hip joint angle, hip joint velocity, SEA torque and power. For each graph the average curve (solid line; blue for left and red for right joint) is shown along with the standard deviation contour. (For interpretation of the references to color in this figure legend, the reader is referred to the web version of this article.)

without hindering its movement. Finally, also in this case there is a quite symmetrical behavior between the right and the left side, the maximum difference for the SEA mean power in the worst scenario **Q10** being (5 km/h) equal to 5%.

4. Discussion

The experiments presented in the previous section aimed at assessing our mechatronic system in static, dynamic and interacting conditions. More specifically, we addressed: (1) the overall system usability as a wearable device physically interfacing with a human subject; (2) the dynamic performance of the low-level torque control; (3) the overall usability of the APO in a prototypical task of walking with a healthy subject wearing the device in both TM and AM modalities.

(1) *Physical human–robot interface*: the orthotic shells coupled with the subject provided a comfortable support and the large interaction area distributed over five contact zones the pressure on user's trunk and thighs. Position and extend of these contact areas actually prevent the physical coupling from being unstable, especially when the actuators deliver high torques. If we compare **Q11** the design with the ones of similar devices (e.g., the HONDA hip support, hip exoskeleton by Ferris et al. [39] and SERKA [35]) we can notice how the attachment points are much smaller, and thus can easily become unstable: a typical problem in exoskeletons is that the motion conveyed from the robot actuated joints to the user limbs goes lost in the slippage of the interaction cuffs, which may tilt around the limb bone and lead to shear stresses and high concentrated loads if they are too thin. In our APO, the rigid structure of the linkages and the soft and adjustable orthotic shells

ensures a correct transmission of relatively high assistive torque values (namely in the range of up to ± 10 N·m) over a wide range of gait velocity: indeed, during the walking task – under AM condition – the healthy volunteer did not report any discomfort from both wearing the device and mechanically interacting with it.

Several passive and lockable DoFs, designed to adjust frame dimensions and linkages positions as well as to align the anatomical rotational axes with the actuated ones, allow to cover a wide range of user's sizes. The resulting structure is however light, with a total weight of 4.2 kg: in future developments of the device, since control electronics and battery pack will be on-board, we expect the global weight to increase up to 5–6 kg. This should not represent a limitation for the device: indeed, as demonstrated by Abe et al. in [50], carrying a 6 kg load on the lower part of the back does not significantly affect the human energy expenditure during a task of ground-level walking.

From the above analysis we derive – as a future perspective for our research activities – the need of experimentally assessing the actual loading effect onto the human body which derives from wearing and walking with the APO (both under TM and AM): this will be done by carrying out measurements of energy consumption by means of an indirect calorimeter.

(2) *Low-level torque control*: the experimental characterization of the low-level control pointed out that the proposed implementation for the SEA and its control system have a suitable dynamic performance to provide an assistive torque with null-to-minimum output impedance.

The step-response experiments pointed out that the tracking capabilities of the device actuator are fast and prompt enough, this feature being mainly a property of the chosen motors and their PID tuning. The chirp response analysis stressed out that the low-level controller leads to a -3 dB control bandwidth of 15.5 Hz, thus broadly enclosing the typical frequencies of human gait. This result is comparable with those attained with another lower-limb device, endowing SEAs and an adaptive-oscillator-based controller, the LOPES platform [51]: the main innovation in this work is that we were able to reach the same performances with a *light-weight and portable* device, while the LOPES is structurally sustained by a treadmill. Finally, within the 0.2–3.2 Hz frequency bandwidth, in zero-torque mode we measured values of parasitic torque and residual stiffness relatively low and comparable with the ones reported in state-of-the-art robots [51].

(3) *Usability for assistive strategy*: the usability of the system as an assistive device has been explored by analyzing and comparing the TM and AM experimental session results (Figs. 8 and 9 respectively): in TM, we assessed the capability of the APO to promptly reject disturbances due to the variability of joint motion, with a peak of resistive torque of 0.4 N·m, while in AM we observed how the system was able to provide a high amount of net positive power, with minimal differences between the joint angle motion profile between the TM and AM conditions (apart from the increased variability over different strides), this being a proof that the APO in AM mode does not affect the natural gait cadence.

The reader should notice that in this paper the efficacy of the device in reducing the user effort has been not directly demonstrated, although the selected algorithm showed capability to reduce the whole-body metabolic consumption of the wearer receiving assistance from the LOPES treadmill-based rehabilitation platform [18]. Indeed, no sensors for measuring physical effort, e.g. EMG electrodes to monitor the muscular activity of the wearer or pressure sensor to record the interaction between the user and the orthotic shells, have been used in the experimental session. Nevertheless, Fig. 9 showed a net positive power flowing through the SEA units: this power is ultimately conveyed to the user's thigh, since the exoskeleton moving linkage is not exchanging actions with any other system. It is reasonable to admit that the

exoskeleton power difference between Figs. 8 and 9 corresponds to the energy the wearer saved, if the power consumption of the global system (user plus exoskeleton) in achieving the walking gait is considered constant between TM and AM. This latter assumption is however not ensured, since a dynamic interaction between the orthosis and the wearer may affect the way the walking is approached (changing its RoM and muscular synergies), but the reported data in Fig. 9 are however indicators of the original device intent, i.e. to supply power in order to assist the gait.

5. Conclusions

In this paper, we presented a novel light-weight bilateral active pelvis exoskeleton for hip flexion–extension assistance. The design of APO addressed main innovative features: a light-weight carbon-fiber structure (a total weight of 4.2 kg) with orthotic shells at the human–robot interface and several passive DoFs for adjustment; a compact SEA with a customized torsional spring that ensures to apply an assistive torque with minimum output impedance. These features satisfy important design requirements for an assistive device: (i) a wide and comfortable human–robot physical interface capable to transmit the assistive torque; (ii) a safe and effective actuation and control systems which avoid additional effort during walking both in TM and AM.

In this paper, the design and development of the system has been described in detail, in association with experimental characterization performed to assess its effectiveness in a prototypical gait-assistance scenario. Future works will focus on three main strands. First, we will carry out a more detailed characterization of the loading effect of APO on the human subject by measuring the user energy expenditure while walking. Second, we will validate the current APO system in a large study with elderly people affected by gait impairment in order to demonstrate the system usability in reducing their effort in tasks of ground-level walking. Finally, we will design and develop an updated version of APO with on-board electronics and battery, and with a better placement of the actuation units which will favor the natural swing of the arms during walking.

Finally, it has been shown how the device applied in TM a near-zero torque to the thigh linkage, independently on the walking phase, while in AM it supplied power to foster the gait. In which relation this latter exoskeleton output power is with the user's effort reduction is an open question, and will be the object of future works: the present study only aimed at explaining and validating the orthotic device and its simple – but effective – gait-adaptive control method.

References

[1] Healthy ageing: keystone for a sustainable Europe, http://ec.europa.eu/health7ph_information/indicators, 2007.

[2] H. Stolze, S. Klebe, C. Baecker, C. Zechlin, L. Friege, S. Pohle, G. Deuschl, Prevalence of gait disorders in hospitalized neurological patients, Mov. Disorders 20 (1) (2005) 89–94.

[3] A.H. Snijders, B.P. van de Warrenburg, N. Giladi, B.R. Bloem, Neurological gait disorders in elderly people: clinical approach and classification, Lancet Neurol. 6 (1) (2007) 63–74.

[4] J. Verghese, A. LeValley, C.B. Hall, M.J. Katz, A.F. Ambrose, R.B. Lipton, Epidemiology of gait disorders in community-residing older adults, J. Am. Geriatr. Soc. 54 (2) (2006) 255–261.

[5] R.S. Wilson, J.A. Schneider, L.A. Beckett, D.A. Evans, D.A. Bennett, Progression of gait disorder and rigidity and risk of death in older persons, Neurology 58 (12) (2002) 1815–1819.

[6] J.A. Ashton-Miller, Age-associated changes in the biomechanics of gait and gait-related falls in older adults, in: J.M. Hausdorff, N.B. Alexander (Eds.), Gait Disorders: Evaluation and Management, Taylor & Francis, Boca Raton, 2005, pp. 63–100.

[7] R. Burge, B. Dawson-Hughes, D.H. Solomon, J.B. Wong, A. King, A. Tosteson, Incidence and economic burden of osteoporosis-related fractures in the United States, 2005–2025, J. Bone Miner. Res. 22 (3) (2007) 465–475.

[8] B.R. Bloem, J. Haan, A.M. Lagaay, W. van Beek, A.R. Wintzen, R.A. Roos, Investigation of gait in elderly subjects over 88 years of age, J. Geriatr. Psychiatry Neurol. 5 (2) (1992) 78–84.

[9] T.D. Fife, R.W. Baloh, Disequilibrium of unknown cause in older people, Ann. Neurol. 34 (5) (1993) 694–702.

[10] G.T. Whitman, T. Tang, A. Lin, R.W. Baloh, A prospective study of cerebral white matter abnormalities in older people with gait dysfunction, Neurology 57 (6) (2001) 990–994.

[11] R.R. Benson, C.R.G. Guttmann, X. Wei, S.K. Warfield, C. Hall, J.A. Schmidt, R. Kikinis, L.I. Wolfson, Older people with impaired mobility have specific loci of periventricular abnormality on MRI, Neurology 58 (1) (2002) 48–55.

[12] R.W. Baloh, S.H. Ying, K.M. Jacobson, A longitudinal study of gait and balance dysfunction in normal older people, Arch. Neurol. 60 (6) (2003) 835–839.

[13] L. Wolfson, X. Wei, C.B. Hall, V. Panzer, D. Wakefield, R.R. Benson, J.A. Schmidt, S.K. Warfield, C.R.G. Guttmann, Accrual of MRI white matter abnormalities in elderly with normal and impaired mobility, J. Neurol. Sci. 232 (1) (2005) 23–27.

[14] A. Kesler, L. Gregory, H. Talia, G. Leor, G. Nir, H. Jeffrey, Shedding light on walking in the dark: the effects of reduced lighting on the gait of older adults with a higher-level gait disorder and controls, J. Neuroeng. Rehabil. 2 (2005) 27.

[15] K.A. Kerber, G.P. Ishiyama, R.W. Baloh, A longitudinal study of oculomotor function in normal older people, Neurobiol. Aging 27 (9) (2006) 1346–1353.

[16] J.L. Pons, Rehabilitation exoskeletal robotics. The promise of an emerging field, IEEE Eng. Med. Biol. Mag. 29 (3) (2010) 57–63.

[17] R. Ronsse, N. Vitiello, T. Lenzi, J. van den Kieboom, M.C. Carrozza, A.J. Ijspeert, Human–robot synchrony: flexible assistance using adaptive oscillators, IEEE Trans. Biomed. Eng. 58 (4) (2011) 1001–1012.

[18] R. Ronsse, T. Lenzi, N. Vitiello, B. Koopman, E. van Asseldonk, S.M.M. De Rossi, J. van den Kieboom, H. van der Kooij, M.C. Carrozza, A.J. Ijspeert, Oscillator-based assistance of cyclical movements: model-based and model-free approaches, Med. Biol. Eng. Comput. 49 (10) (2011) 1173–1185.

[19] A.M. Dollar, H. Herr, Lower extremity exoskeletons and active orthoses: challenges and state-of-the-art, IEEE Trans. Robot. 24 (1) (2008) 144–158.

[20] A. Schiele, F.C. van der Helm, Kinematic design to improve ergonomics in human machine interaction, IEEE Trans. Neural Syst. Rehabil. Eng 14 (4) (2006) 456–469.

[21] A.H.A. Stienen, E.E.G. Hekman, F.C.T. van der Helm, H. van der Kooij, Self-aligning exoskeleton axes through decoupling of joint rotations and translations, IEEE Trans. Robot. 25 (3) (2009) 628–633.

[22] E. Rocon, J.M. Belda-Lois, A.F. Ruiz, M. Manto, J.C. Moreno, J.L. Pons, Design and validation of a rehabilitation robotic exoskeleton for tremor assessment and suppression, IEEE Trans. Neural Syst. Rehabil. Eng. 15 (3) (2007) 367–378.

[23] G.A. Pratt, M.M. Williamson, Series elastic actuators, in: Proceedings IEEE/RSJ International Conference on Intelligent Robots and Systems. Human Robot Interaction and Cooperative Robots, vol. 1, Aug. 1995, pp. 399–406.

[24] S.K. Banala, S.H. Kim, S.K. Agrawal, J.P. Scholz, Robot assisted gait training with active leg exoskeleton (ALEX), IEEE Trans. Neural Syst. Rehabil. Eng. 17 (1) (2009) 2–8.

[25] G.S. Sawicki, K.E. Gordon, D.P. Ferris, Powered Lower limb orthoses: applications in motor adaptation and rehabilitation, in: 9th International Conference on Rehabilitation Robotics, Jun. 2005, pp. 206–211.

[26] P. Beyl, M. Van Damme, R. Van Ham, B. Vanderborght, D. Lefeber, Design and control of a lower limb exoskeleton for robot-assisted gait training, ~~Appl. Bionics Biomech.~~ 6 (2) (2009) 229–243.

[27] S. Jezernik, G. Colombo, T. Keller, H. Frueh, M. Morari, Robotic orthosis lokomat: a rehabilitation and research tool, Neuromodulation 6 (2) (2003) 108–115.

[28] J.F. Veneman, R. Kruidhof, E.E.G. Hekman, R. Ekkelenkamp, E.H.F. Van Asseldonk, H. van der Kooij, Design and evaluation of the LOPES exoskeleton robot for interactive gait rehabilitation, IEEE Trans. Neural Syst. Rehabil. Eng. 15 (3) (2007) 379–386.

[29] R.J. Farris, H.A. Quintero, M. Goldfarb, Preliminary evaluation of a powered lower limb orthosis to aid walking in paraplegic individuals, IEEE Trans. Neural Syst. Rehabil. Eng. 19 (6) (2011) 652–659.

[30] H. Kawamoto, T. Hayashi, T. Sakurai, K. Eguchi, Y. Sankai, Development of single leg version of HAL for hemiplegia, in: Conf. Proc. IEEE Eng. Med. Biol. Soc., vol. 2009, Jan. 2009, pp. 5038–5043.

[31] K. Kong, D. Jeon, Design and control of an exoskeleton for the elderly and patients, IEEE/ASME Trans. Mechatronics 11 (4) (2006) 428–432.

[32] S. Krut, M. Benoit, E. Dombre, F. Pierrot, MoonWalker, a lower limb exoskeleton able to sustain bodyweight using a passive force balancer, in: Proceedings IEEE International Conference on Robotics and Automation, May 2010, pp. 2215–2220.

[33] H. Kazerooni, R. Steger, The Berkeley lower extremity exoskeleton, J. Dyn. Syst., Meas. Control 128 (1) (2006) 14–25.

[34] C.J. Walsh, K. Pasch, H. Herr, An autonomous, underactuated exoskeleton for load-carrying augmentation, in: Proc. IEEE/RSJ Int. Conf. Intell. Robots Syst. (IROS), Beijing, China, 2006, pp. 1410–1415.

[35] J.S. Sulzer, R.A. Roiz, M.A. Peshkin, J.L. Patton, A highly backdrivable, lightweight knee actuator for investigating gait in stroke, IEEE Trans. Robot. 25 (3) (2009) 539–548.

[36] J. Hitt, A.M. Oymagil, T. Sugar, K. Hollander, A. Boehler, J. Fleeger, Dynamically Controlled Ankle–Foot Orthosis (DCO) with regenerative kinetics: incrementally attaining user portability, in: Proceedings IEEE International Conference on Robotics and Automation, Apr 2007, pp. 1541–1546.

[37] J.A. Blaya, H. Herr, Adaptive control of a variable-impedance ankle–foot orthosis to assist drop-foot gait, IEEE Trans. Neural Syst. Rehabil. Eng. 12 (1) (2004) 24–31.

[38] B.G. do Nascimento, C.B.S. Vimieiro, D.A.P. Nagem, M. Pinotti, Hip orthosis powered by pneumatic artificial muscle: voluntary activation in absence of myoelectrical signal, Artif. Organs 32 (4) (2008) 317–322.

[39] D.P. Ferris, C.L. Lewis, Robotic lower limb exoskeletons using proportional myoelectric control, in: Conf. Proc. IEEE Eng. Med. Biol. Soc., vol. 2009, Jan. 2009, pp. 2119–2124.

[40] F. Giovacchini, M. Fantozzi, M. Peroni, M. Moisé, M. Cempini, M. Cortese, D. Lefeber, M.C. Carrozza, N. Vitiello, A light-weight exoskeleton for hip flexion-extension assistance, in: International Congress on Neurotechnology. Electronics and Informatics, Sept. 2013, pp. 194–198.

[41] N. Vitiello, T. Lenzi, S. Roccella, S.M.M. De Rossi, E. Cattin, F. Giovacchini, F. Vecchi, M.C. Carrozza, NEUROExos: a powered elbow exoskeleton for physical rehabilitation, IEEE Trans. Robot. 29 (1) (2013) 220–235.

[42] J.F. Veneman, A series elastic- and Bowden-cable-based actuation system for use as torque actuator in exoskeleton-type robots, Int. J. Robot. Res. 25 (3) (2006) 261–281.

[43] M. Zinn, O. Khatib, B. Roth, A new actuation approach for human friendly robot design, in: Proceedings IEEE International Conference on Robotics and Automation, vol. 1, Vol.1, Apr. 2004, pp. 249–254.

[44] D.A. Winter, Biomechanics and Motor Control of Human Movement, John Wiley & Sons, 2009, p. 370.

[45] C.J. Walsh, K. Endo, H. Herr, A quasi-passive legacy exoskeleton for load-carrying augmentation, Int. J. Hum. Robot. 4 (3) (2007) 487–506.

[46] M. Cempini, F. Giovacchini, N. Vitiello, M. Cortese, M. Moisé, F. Posteraro, M.C. Carrozza, NEUROExos: a powered elbow orthosis for post-stroke early neurorehabilitation, in: Conf. Proc. IEEE Eng. Med. Biol. Soc., vol. 2013, Jan. 2013, pp. 342–345.

[47] L. Righetti, J. Buchli, A.J. Ijspeert, Dynamic Hebbian learning in adaptive frequency oscillators, Phys. D 216 (2) (2006) 269–281.

[48] R. Ronsse, S.M.M. De Rossi, N. Vitiello, T. Lenzi, M.C. Carrozza, A.J. Ijspeert, Real-time estimate of velocity and acceleration of quasi-periodic signals using adaptive oscillators, IEEE Trans. Robot. 29 (3) (2013) 783–791.

[49] R. Ronsse, B. Koopman, N. Vitiello, T. Lenzi, S.M.M. De Rossi, J. van den Kieboom, E. van Asseldonk, M.C. Carrozza, H. van der Kooij, A.J. Ijspeert, Oscillator-based walking assistance: a model-free approach, in: IEEE Int. Conf. Rehabil. Robot., Jan. 2011, pp. 597–5352.

[50] D. Abe, K. Yanagawa, S. Niihata, Effects of load carriage, load position, and walking speed on energy cost of walking, Appl. Ergon. 35 (4) (2004) 329–335.

[51] H. Vallery, R. Ekkelenkamp, H. van der Kooij, M. Buss, Passive and accurate torque control of series elastic actuators, in: IEEE/RSJ International Conference on Intelligent Robots and Systems, Nov. 2007, pp. 3534–3538.

Francesco Giovacchini was born in Pisa, Italy, in 1980. He received his B.Sc. in Mechanical Engineering and his M.Sc. in Mechanical Engineering from the University of Pisa in 2003 and in 2006 respectively. Starting from 2007 he is a research assistant at The BioRobotics Institute (ex ARTS Lab) of Scuola Superiore Sant'Anna. His research interests are in the fields of biomechatronics with particular interests in robotic platforms and wearable devices for rehabilitation and assistance (i.e. exoskeleton for the hand and for the upper and lower limbs).

Federica Vannetti received the M.Sc. degree in Biomedical Engineering in 2005 and the Ph.D. in Mechanical Design in 2010, from University of Florence, Italy. In 2009–2010 she has been a ~~post-Doc~~ at the Laboratory of Industrial Bioengineering, University of Florence, Italy, working on the infrared thermography applied to ophthalmology. Her research interest is in the field of gait analysis by using motion capture, markerless system, inertial sensor and EMG signals; furthermore she is involved in some research work about metabolic consumption in healthy and pathological subjects. She ~~works~~ at Don Gnocchi Foundation as a researcher since 2010.

Matteo Fantozzi was born in Viareggio, Italy, in 1981. He received his B.Sc. in Aerospace Engineering and his M.Sc. in Aerospace Engineering in 2006 and 2011 respectively. In 2007 he worked at Fosber S.p.a. (Monsagrati, Italy) – Company producer of machines for the corrugated paper sector – as a mechanical engineer. From November 2011 to March 2012 he worked for Velan ABV S.p.a. (Lucca, Italy), a Company producer of valves and actuation systems for the oil&gas sector. Starting from April 2012 he is a research assistant at The BioRobotics Institute of Scuola Superiore Sant'Anna. His research interests are in the field of mechanics, especially in innovative mechanical solutions, and in the field of space propulsion with particular interests in electric propulsion (plasma thrusters).

Marco Cempini received the M.Sc. degree in aeronautical engineering (cum laude) both from the University of Pisa, Italy and from Scuola Superiore Sant'Anna, Pisa, Italy in 2010. He is currently working towards the Ph.D. degree in Biorobotics at The BioRobotics Institute, Scuola Superiore Sant'Anna, Pisa, Italy, and he is a Visiting Student at the Robotics and Mechatronics Laboratory of University of Twente, Enschede, Netherlands. His current research interests include mechanical design, modeling and development for wearable robotics, oriented towards the upper and lower limb assistance. From 2011 Mr. Cempini is a student member of IEEE, RAS and EMBS scientific societies, and from 2012 of ASME. In 2008, he participated in the first ESA Lunar Robotics Challenge as a master student.

Mario Cortese received his M.Sc. in Electronic Engineering (cum laude) in 2011. He is currently a Ph.D. student in Biorobotics at The BioRobotics Institute, Scuola Superiore Sant'Anna, Pisa, Italy. His current research interest includes electronic design for wearable robotics, developing of human–robot interfaces and control strategies for upper and lower limb rehabilitation robots.

Andrea Parri received the B.Sc. degree in biomedical engineering from University of Pisa, Italy, in 2011. He is currently a master student at the University of Pisa and he is working on his master thesis at The BioRobotics Institute. His major research interest is in the development of adaptive assistive strategies for wearable robots.

Tingfang Yan is currently a Ph.D. student of The Biorobotics Institute, Scuola Superiore Sant'Anna, Pisa, Italy. She received her B. Sc. degree in Control Science and Engineering from Shandong University, China in 2011. Her main research interests include the development of wearable robotic devices for human motion assistance and rehabilitation.

Dirk Lefeber received the degree in Study of Civil Engineering at the Vrije Universiteit Brussel and a Ph.D. in Applied Sciences, Vrije Universiteit Brussel, in 1986. Currently he is a professor at the Dept. of Mechanical Engineering and the head of the Robotics and Multibody Mechanics Research Group, Vrije Universiteit Brussel. His research interests are new actuators with adaptable compliance, dynamically balanced robots, robot assistants, rehabilitation robotics and multibody dynamics.

Nicola Vitiello received the M.Sc. degree in Biomedical Engineering (cum laude) from the University of Pisa, Italy, in 2006, and from Scuola Superiore Sant'Anna, Pisa, Italy, in 2007. He also received the Ph.D. degree in Biorobotics from the Scuola Superiore Sant'Anna, Pisa, Italy, in 2010. He is currently an Assistant Professor with The BioRobotics Institute, Scuola Superiore Sant'Anna. He is the author or co-author of 21 ISI/Scopus papers and 30 peer-review conference proceedings papers. He has served as the Scientific Secretary of the EU FP7 CA-RoboCom project, and he is currently the Project Coordinator of: the EU FP7 CYBERLEGs Project, the IUVO Project funded by Fondazione Pisa, and the EARLYREHAB Project funded by Regione Toscana. His main research interests include the development of wearable robotic devices for human motion assistance and rehabilitation and of robotic platforms for neuroscientific investigations.